Photodissociation of allyl-d_2 iodide excited at 193 nm: Stability of highly rotationally excited H_2CDCH_2 radicals to C–D fission

D. E. Szpunar, Y. Liu, M. J. McCullagh, and L. J. Butler[a)]
The James Franck Institute and Department of Chemistry, The University of Chicago, Chicago, Illinois 60637

J. Shu
Chemical Sciences Division, Lawrence Berkeley National Laboratory, Berkeley, California 94720

(Received 19 May 2003; accepted 10 June 2003)

The photodissociation of allyl-d_2 iodide ($H_2C=CDCH_2I$) and the dynamics of the nascent allyl-d_2 radical (H_2CCDCH_2) were studied using photofragment translational spectroscopy. A previous study found the allyl radical stable at internal energies up to 15 kcal/mol higher than the 60 kcal/mol barrier to allene+H formation as the result of a centrifugal barrier. The deuterated allyl radical should then also show a stability to secondary dissociation at internal energies well above the barrier due to centrifugal effects. A comparison in this paper shows the allyl-d_2 radical is stable to allene+D formation at energies of 2–3 kcal/mol higher than that of the nondeuterated allyl radical following photolysis of allyl iodide at 193 nm. This is most likely a result of a combination of the slight raising of the barrier from the difference in zero-point levels and a reduction of the impact parameter of the dissociative fragments due to the decrease in frequency of the C–D bending modes, and therefore allene+D product orbital angular momentum, $|\vec{L}|=\mu|\vec{v}_{rel}|b$. The integrated signal taken at $m/e=40$ (allene) and $m/e=41$ (allene-d_1 and propyne-d_3) shows a minor fraction of the allyl-d_2 radicals isomerize to the 2-propenyl radical, in qualitative support of earlier conclusions of the domination of direct allene+H formation over isomerization. © *2003 American Institute of Physics.* [DOI: 10.1063/1.1596853]

INTRODUCTION

The dissociation dynamics of the allyl radical has been the topic of many studies in the past.[1–7] The work presented here uses a technique developed to study the unimolecular dissociation channels of isomerically selected radicals[8] in continuation of a previous study in which allyl iodide was used as a photolytic precursor of the allyl radical.[7] Unlike the other prior studies on allyl radicals, these studies examine the dissociation dynamics of highly rotationally excited allyl radicals. C–I bond fission producing iodine in its ground, $I(^2P_{3/2})$, and excited, $I(^2P_{1/2})$, spin–orbit state were found to be the only major channels upon photolysis of allyl iodide at 193 nm. The nascent allyl radicals were dispersed by their translational energy, allowing the dynamics of the allyl radical to be studied as a function of its internal energy. All of the $I(^2P_{3/2})$ formation channel allyl radicals were found to have enough internal energy to undergo C–H bond fission, primarily forming allene ($H_2C=C=CH_2$)+H. No significant isomerization to the 2-propenyl radical was detected at the internal energies accessed in these experiments. Only a fraction of the $I(^2P_{1/2})$ formation channel allyl radicals had sufficient energy to overcome the 60 kcal/mol barrier[9] to allene+H formation, leaving some stable allyl radicals to be detected at $m/e=41$. It was found, however, that a considerable fraction of the allyl radicals was stable to dissociation at energies up to 15 kcal/mol higher than expected. This stability was attributed to a centrifugal barrier produced by significant partitioning of rotational energy to the allyl radical in the primary photolysis step. The conservation of angular momentum along with the small reduced mass, μ, and near zero impact parameter, b, characterizing the radical's dissociation caused most of the allyl radical angular momentum to be partitioned to allene rotation because the orbital angular momentum of the scattered allene+H products, $|\vec{L}|=\mu|\vec{v}_{rel}|b$, is required to be small. This introduces a centrifugal barrier that prohibits the dissociation of rotationally excited allyl radicals even though their internal energy is well in excess of the 60 kcal/mol barrier.

The results presented here are a continuation of this study. We used photofragment translational spectroscopy to characterize the photodissociation of allyl-d_2 iodide ($H_2C=CDCH_2I$; see Fig. 1) excited at 193 nm and compare it to newly obtained nondeuterated allyl iodide photolysis data. As mentioned earlier, the nascent allyl radical produced through the 193 nm photolysis of allyl iodide has enough internal energy to undergo C–H bond fission, producing either allene or propyne through two main pathways.[7] The first pathway (60 kcal/mol barrier height[9]) is direct allene formation, where the central H atom is lost in one step. The second produces either allene (57.5 kcal/mol barrier height[9]) or propyne (56.5 kcal/mol barrier height[9]) following isomerization to the 2-propenyl radical (63.8 kcal/mol barrier height[9]). (The barrier heights quoted here are calculated in Ref. 9 for the nondeuterated species.) The reactions of interest for the allyl-d_2 radical are shown in reactions (1)–(4).

a)Electronic mail: l-butler@uchicago.edu

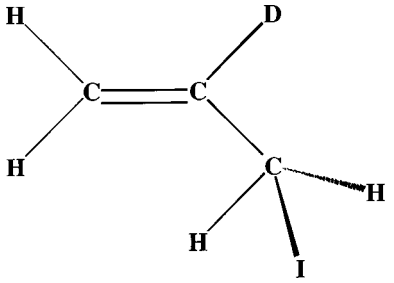

FIG. 1. Allyl-d_2 iodide.

$$CH_2CDCH_2 \rightarrow D + CH_2{=}C{=}CH_2 \quad \text{(allene, mass = 40)} \tag{1}$$

$$CH_2CDCH_2 \rightarrow H_2DCC{=}CH_2 \quad \text{(2-propenyl radical)}$$

$$\rightarrow H + H_2DCC{\equiv}CH$$

$$\text{(propyne-}d_3\text{, mass = 41)} \tag{2}$$

$$\rightarrow D + CH_2{=}C{=}CH_2$$

$$\text{(allene, mass = 40)} \tag{3}$$

$$\rightarrow H + CHD{=}C{=}CH_2$$

$$\text{(allene-}d_1\text{, mass = 41).} \tag{4}$$

The major nondeuterated allyl radical dissociation product was identified in the prior work as allene based on the appearance of signal (at 9.6 eV compared to an allene ionization energy[10] of 9.7 eV and propyne ionization energy[10] of 10.36 eV) and slope of a photoionization efficiency (PIE) curve.[7] In this work, replacing the central hydrogen with a deuterium atom (Fig. 1) can facilitate allyl radical H-loss channel identification without relying on PIE curves. As can be seen, direct allene formation [reaction (1)] will result only in mass 40 products. Isomerization to the 2-propenyl radical can give either mass 40 or mass 41 allene products [reactions (3), (4)] while propyne formation following isomerization to the 2-propenyl radical results only in deuterated propyne [mass 41, reaction (2)].

Changing the central hydrogen to deuterium will increase the orbital angular momentum of the allene+H products, $|\vec{L}| = \mu |\vec{v}_{rel}| b$, due to the increase in reduced mass for a deuterium loss reaction. However, the impact parameter and zero-point-corrected barrier height can also be changed upon the replacement of hydrogen with deuterium. In this study we probe the effect of these competing factors on the stability of rotationally excited allyl radicals.

EXPERIMENT

The results presented were taken on the rotatable-source, fixed-detector, crossed-laser molecular beam apparatus at the Advanced Light Source at the Lawrence Berkeley National Laboratory.[11] Briefly, either allyl-d_2 iodide, or nondeuterated allyl iodide, was placed in a bubbler at 0 °C through which He gas was bubbled to give a total backing pressure of 500 Torr. A 0.5 mm piezo-valve nozzle was kept at a temperature of 80–95 °C to reduce clustering. The molecular beam was crossed with the pulsed light from an ArF filled Lambda Physik COMPex 110 excimer laser operating near 3 mJ/

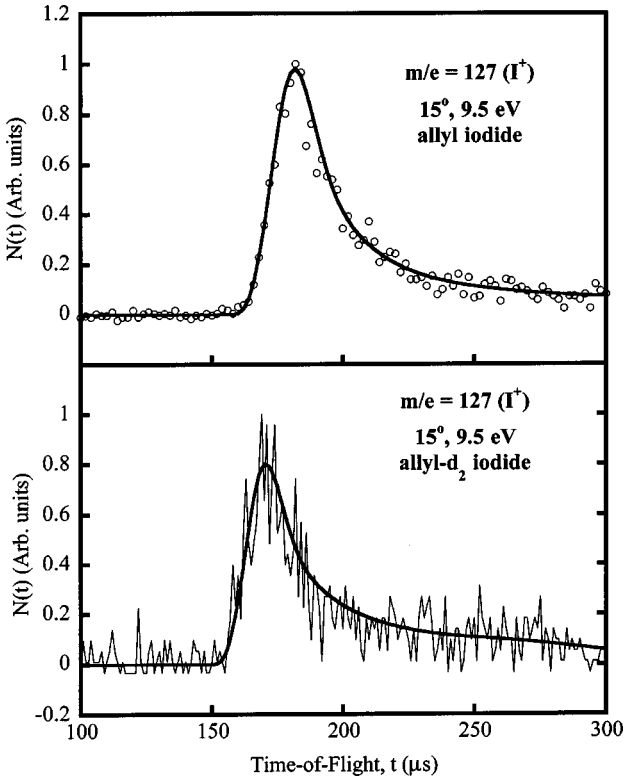

FIG. 2. Time-of-flight taken at $m/e = 127$ (I^+), a source angle of 15° and a photoionization energy of 9.5 eV. The top panel is from nondeuterated allyl iodide photolysis and the bottom panel is from allyl-d_2 iodide photolysis. As the I ($^2P_{3/2}$) ionization energy is 10.45 eV, this signal is due to the I ($^2P_{1/2}$) formation channel only.

pulse and focused to a 2×5 mm cross sectional area in the interaction region. The resulting photofragments with lab velocities along the detector axis flew 15.2 cm to the ionization region where they were photoionized using tunable synchrotron radiation. The ions were then mass selected using a quadrupole mass filter and detected with a Daly detector.[12] A synchrotron aperture of 10×10 mm was used, and the radiation passed through a 1 mm thick MgF_2 filter (as opposed to the 2 mm filter used previously[7]) for all data shown. The synchrotron radiation has been recently recalibrated[13] so the photoionization energy in each spectrum in this paper is more accurate than in papers from this beamline before 2003. The undulator gap (mm) was calculated from the required photoionization energy, x (eV), using the following polynomial:

$$\text{gap(mm)} = 7.875(\text{mm}) + 2.5054(\text{mm/eV})x - 0.068\,545(\text{mm/eV}^2)x^2 + 0.000\,824\,77(\text{mm/eV}^3)x^3.$$

The background-subtracted time-of-flights shown in the figures include ion flight time, with the fits corrected using an ion flight constant of 6.5 μs(amu)$^{-1/2}$ determined through SF_6 time-of-flights in the week that the data were taken.

The synthesis of allyl-d_2 iodide was adapted from that of Minsek and Chen.[14] First, 6.484 g (0.1545 mol) lithium aluminum deuteride and 240 ml of ethyl ether were placed in a 500 ml three neck flask, stirred under dry nitrogen, and

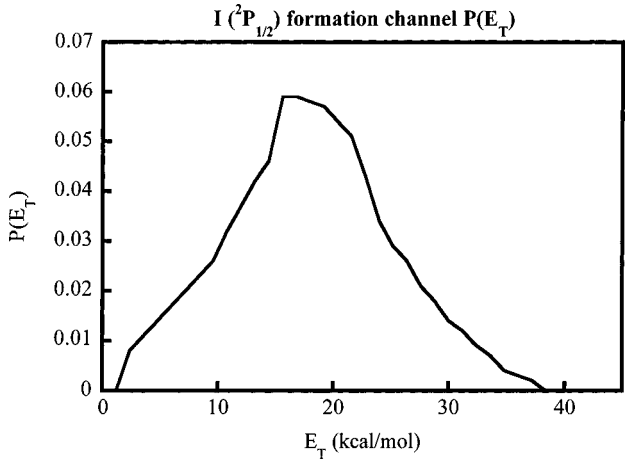

FIG. 3. Translational energy distribution $[P(E_T)]$ derived from the forward convolution fit of the $I(^2P_{1/2})m/e=127$ spectra shown in Fig. 2. It ranges from 1.2–38.4 kcal/mol, corresponding to an internal energy range, E_{int}, of $45.2<E_{\text{int}}<83.6$ kcal/mol in the nascent allyl radical.

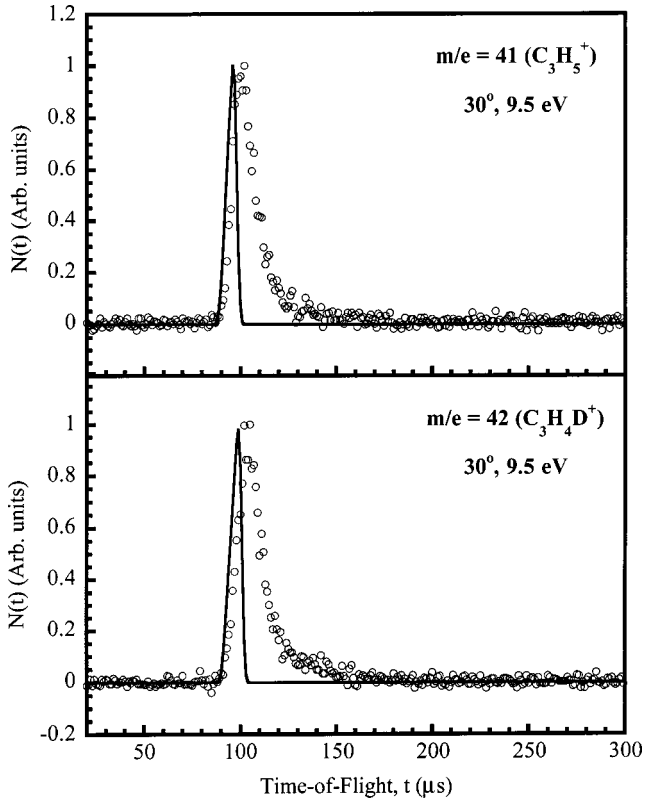

FIG. 4. Allyl radical time-of-flights taken at a source angle of 30° and a photoionization energy of 9.5 eV. The top panel is the time-of-flight of nondeuterated allyl radicals ($m/e=41$) from allyl iodide photodissociation and the solid line is the fit predicted when the $I(^2P_{1/2})P(E_T)$ (Fig. 3) is truncated at the 60 kcal/mol barrier to allene+H formation. The bottom panel is the time-of-flight of allyl-d_2 radicals ($m/e=42$) and the solid line is the fit predicted from the 61.5 kcal/mol barrier to allene+D formation.

then cooled in an ice bath for 30 minutes. Over four hours, 8.44 ml (0.144 mol) of propargyl alcohol were added. The reaction was allowed to stir overnight at room temperature and then refluxed for 2.5 hours (at 45 °C). The reaction was cooled in an ice bath, quenched by the addition of 8.43 ml (0.468 mol) of deionized water and then the mixture was filtered through celite, removing the white precipitate. Both the flask and the celite were washed with ether, the remaining clear liquid was distilled at room temperature under house vacuum to remove most of the ether and then distilled at atmospheric pressure to yield 1.965 g (0.033 mol, 23% yield) of allyl-d_2 alcohol. The product distilled over at 97 °C as a clear liquid. ^{1}H NMR (400 MHz, $CDCl_3$) δ 4.16 (m), 5.15 (m), 5.28 (m).

The 1.508 g of allyl-d_2 alcohol was placed in a three neck 500 ml round bottomed flask, put under dry nitrogen and 10.2 g (8.65 ml, 0.033 mol) of triphenylphosphite was added via syringe. 7.12 g (3.12 ml, 0.050 mol) of methyl iodide was then added dropwise through a syringe over five minutes. The solution was then heated at reflux (at 80 °C) for 24 hrs. After reflux, the solution was distilled at reduced pressure (house vacuum) into a dry ice and ethanol cooled receiver. This yielded a solution of allyl-d_2 iodide and methyl iodide. The majority of the methyl iodide was then removed by distillation at room temperature under low pressure (house vacuum) for 10 seconds yielding 1.60 g of allyl-d_2 iodide. ^{1}H NMR (400 MHz, $CDCl_3$) δ 3.86 (d), 4.97 (d), 5.24 (m). Because the same $P(E_T)$ was used to fit the $I(^2P_{1/2})$ spectra from both nondeuterated and allyl-d_2 iodide photolysis, as will be shown in the next section, it is not believed that the methyl iodide impurity posed any problems in the experiments.

RESULTS AND ANALYSIS

Figure 2 shows the $m/e=127$ spectrum (I^+) from the photodissociation of nondeuterated allyl iodide (top panel) and from allyl-d_2 iodide photolysis (bottom panel) taken at a source angle of 15° and a photoionization energy of 9.5 eV. As this is taken at an ionization energy below the 10.45 eV ionization energy[10] of $I(^2P_{3/2})$, the signal seen is due to the ionization of $I(^2P_{1/2})$ from the minor $I(^2P_{1/2})$+allyl radical primary product channel. The same translational energy distribution, $P(E_T)$, was used to fit both spectra, as no difference was apparent within the allyl-d_2 iodide $m/e=127$ spectrum's poor signal-to-noise. The $P(E_T)$ derived from the forward convolution fit to Fig. 2 is shown in Fig. 3. Note that although it spans roughly the same translational energy range, it is quantitatively quite different from the previously obtained $I(^2P_{1/2})$ formation channel $P(E_T)$.[7] This might be due to clusters in the previous data, as were thought to be present. Through the conservation of energy, it is noted that the $I(^2P_{1/2})$ formation $P(E_T)$ leaves nascent allyl radicals with an internal energy, E_{int}, of $45.2<E_{\text{int}}<83.6$ kcal/mol.

As previously noted, this energy range should leave a fraction of the nascent allyl radicals stable to allene+H/D formation. Calculations were performed at the G3(B3LYP) level of theory to determine the magnitude of the barrier introduced by the zero-point-energy differences of the nondeuterated and deuterated allyl radicals. An additional barrier of 1.5 kcal/mol was found due to this isotope effect. [The barrier to dissociation of the nondeuterated allyl radical was found to be 59.8 kcal/mol at the G3(B3LYP) level of theory, in agreement with the 60 kcal/mol barrier of Davis *et al.* calculated at the G2(B3LYP) level of theory.[9]] Data were

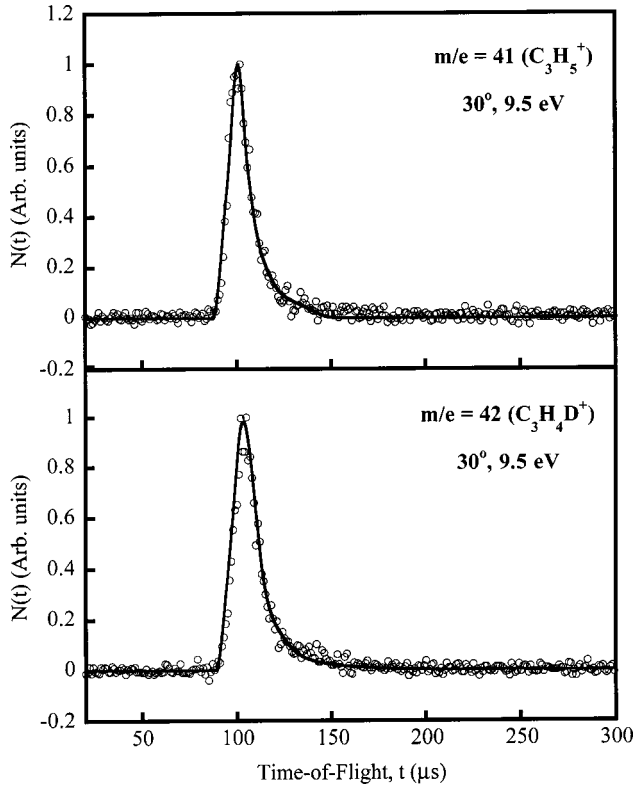

FIG. 5. Allyl radical time-of-flights taken at a source angle of 30° and a photoionization energy of 9.5 eV. The top panel is the time-of-flight of nondeuterated allyl radicals ($m/e=41$) from allyl iodide photodissociation and the bottom of allyl-d_2 radicals ($m/e=42$). The modified $I(^2P_{1/2})P(E_T)$'s used to fit the time-of-flights are shown in Fig. 6.

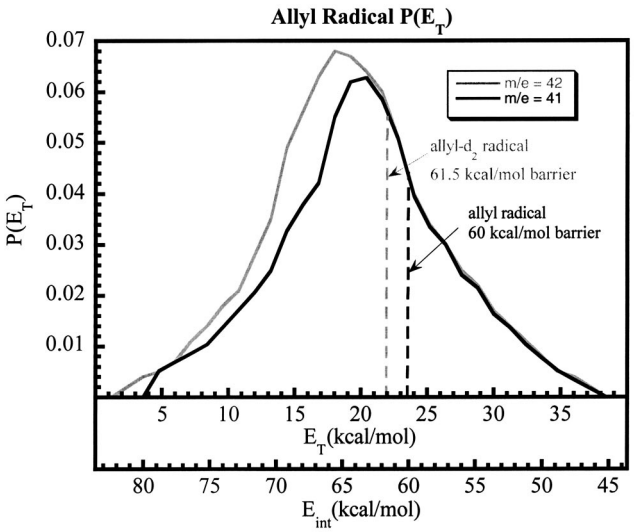

FIG. 6. The $P(E_T)$'s derived from the forward convolution fits to the allyl radical time-of-flights shown in Fig. 5. The black line is the nondeuterated allyl radical $P(E_T)(m/e=41)$ and the gray line is the allyl-d_2 radical $P(E_T)$ $(m/e=42)$. The top *x*-axis is translational energy, the bottom *x*-axis is the corresponding allyl radical internal energy, and the black dotted line marks the 60 kcal/mol barrier to allene+H formation while the gray dotted line marks the 61.5 kcal/mol barrier to allene+D formation.

taken at $m/e=41$ (allyl radical from nondeuterated allyl iodide photolysis) and $m/e=42$ (allyl-d_2 radical) to determine the energy range at which the allyl radicals are stable to dissociation. Figure 4 displays allyl radical spectra taken at a 30° source angle and a photoionization energy of 9.5 eV. The top panel shows the $m/e=41$ allyl radical spectrum from nondeuterated allyl iodide photolysis along with a fit corresponding to the $I(^2P_{1/2})$ formation channel $P(E_T)$ (Fig. 3) truncated at the zero-point-corrected 60 kcal/mol barrier. The bottom panel shows the $m/e=42$ allyl radical from allyl-d_2 iodide photolysis along with a fit predicted by its corresponding zero-point-corrected 61.5 kcal/mol barrier. Clearly, both nondeuterated as well as deuterated allyl radical fragments are stable at energies much higher than their respective barriers. As in the previous study, we note that this is due to centrifugal effects. Figure 5 again displays the allyl radical spectra shown in Fig. 4, this time with proper fits. The top panel shows the $m/e=41$ allyl radical spectrum along with its forward convolution fit and the bottom the $m/e=42$ allyl-d_2 radical spectrum with its corresponding fit. In both cases, the translational energy distributions derived in the forward convolution fits are obtained from the $P(E_T)$ for $I(^2P_{1/2})$ formation (Fig. 3) but with the low translational energy side of the $P(E_T)$ lowered until the remainder fit the surviving radical data shown in Fig. 5. The resulting $P(E_T)$'s which fit the surviving momentum-matched allyl radicals in Fig. 5 are shown in Fig. 6, and represent all the $I(^2P_{1/2})$ + allyl radical channel products which produce allyl radicals stable to secondary dissociation. The top *x*-axis in Fig. 6 is the measured translational energy imparted in the dissociation, while the lower *x*-axis is the corresponding internal energy of the allyl radical. The black/gray dotted line marks the 60/61.5 kcal/mol barrier to allene+H/D formation. As can be seen, the $m/e=42$ (gray) distribution survives at internal energies around 2–3 kcal/mol higher than the $m/e=41$ (black) distribution. We will return to this in the Discussion section.

To help determine if the C–H(D) fission occurs directly or after isomerization to the 2-propenyl radical, data were taken at $m/e=40$ and $m/e=41$ from allyl-d_2 iodide photodissociation. Figure 7 shows data taken at $m/e=40$ (allene) at a source angle of 30° and photoionization energy of 10.8 eV. The fit shown is calculated using the $P(E_T)$ derived from the forward convolution fit to I^+ $(m/e=127)$ data from nondeuterated allyl iodide photolysis taken with 200 eV electron-impact ionization (Fig. 2 of Ref. 7), as there are no electron-impact data available from deuterated allyl iodide photolysis. Our previous work showed that $m/e=40$ data would not momentum match with I^+ spectra taken at the photoionization energies (10.8, 12.0 eV) attempted at the synchrotron, even though they are above the ionization energies of both spin–orbit states. This is attributed to the differences in $I(^2P_{3/2})$ and $I(^2P_{1/2})$ photoionization cross sections at these lower ionization energies.

Isomerization to the 2-propenyl radical can give both a propyne product as well as an indirect allene product, and when the allyl-d_2 iodide is used as the precursor both of these indirect channels can result in mass 41 propyne and allene production. The spectrum of $m/e=41$, taken at a source angle of 30° and photoionization energy of 10.8 eV, is shown in Fig. 8.

The fit shown is also calculated from the 200 eV electron-impact ionization $m/e=127$ $P(E_T)$ describing C–I

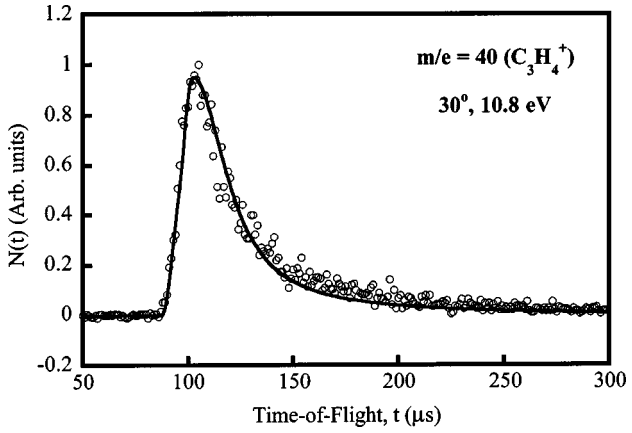

FIG. 7. Time-of-flight at $m/e=40$ ($C_3H_4^+$) corresponding to both direct [reaction (1)] and indirect [reaction (3)] allene formation from allyl-d_2 radical dissociation taken at a source angle of 30° and a photoionization energy of 10.8 eV. It is fit with the $P(E_T)$ derived from the forward convolution fit to the $m/e=127$ (I^+) spectrum (Fig. 2, Ref. 7) of the 193 nm photolysis of nondeuterated allyl iodide taken with 200 eV electron impact ionization as the different photoionization cross sections for $I(^2P_{3/2})$ and $I(^2P_{1/2})$ at the lower photoionization energies used at the synchrotron (10.8, 12.0 eV) prevent a suitable momentum match with $m/e=40$ fragments.

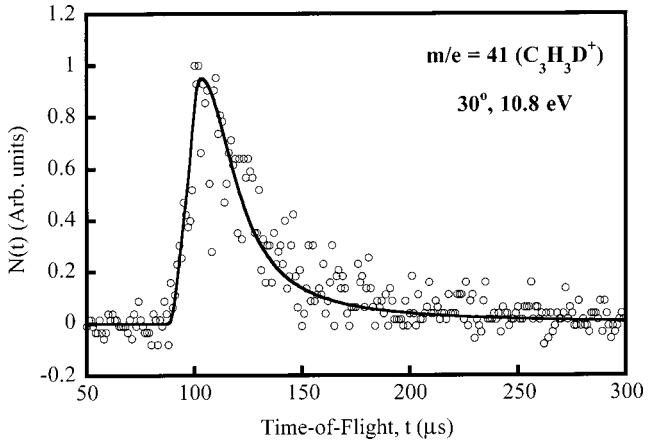

FIG. 8. Time-of-flight at $m/e=41$ ($C_3H_3D^+$) corresponding to indirect propyne [reaction (2)] and allene [reaction (4)] from allyl-d_2 radical dissociation taken at a source angle of 30° and a photoionization energy of 10.8 eV. It is also fit with the $P(E_T)$ derived from the forward convolution fit to $m/e=127$ (I^+) spectra of the 193 nm photolysis of nondeuterated allyl iodide taken with 200 eV electron impact ionization (Fig. 2, Ref. 7).

bond fission of nondeuterated allyl iodide (Fig. 2 of Ref. 7). Unfortunately, the limited sample available prevented the collection of a spectrum with better signal-to-noise. Figure 9 shows $m/e=40$ (black) and $m/e=41$ (gray) spectra from allyl-d_2 iodide photodissociation overlaid, both taken with a source angle of 30° and a photoionization energy of 10.8 eV over 50 000 shots. Integration of the signal from 86–225 μs gives a $m/e=40/41$ ratio of 4.5. We will return to this in the Discussion.

DISCUSSION

The portions shown in Fig. 6 of the $I(^2P_{1/2})$ formation channel $P(E_T)$ (Fig. 3) that fit the surviving nondeuterated allyl radical as well as allyl-d_2 radical spectra show a stability of some highly rotationally excited allyl radicals at internal energies higher than the 60/61.5 kcal/mol barrier to allene+H/D formation. Because the allyl radical loses an H or a D atom from the center carbon, the rotational energy of the allyl radical must appear predominantly as allene product rotational energy as the exit orbital angular momentum of the departing H/D+allene fragments, $|\vec{L}|=\mu|\vec{v}_{rel}|b$, is required to be small. One can see from the comparison of the $P(E_T)$ describing the formation of all nascent allyl radicals (Fig. 3) to that of those events that produce stable allyl radicals (Fig. 6) that the probability of an allyl radical undergoing secondary dissociation depends on its rotational energy, but the allyl-d_2 radical shows a higher survival probability than the nondeuterated allyl radical at the same total internal energy. For example, when allyl radicals are produced from a C–I bond fission event that partitions 18 kcal/mol in product recoil of the allyl radical and $I(^2P_{1/2})$ fragments, the allyl radicals are produced with a total internal energy of 65.6 kcal/mol. The $P(E_T)$'s in Fig. 6 show that about 80% of the H_2CCHCH_2 radicals with this total internal energy survives secondary dissociation, while a considerably larger fraction of the H_2CCDCH_2 radical survives secondary dissociation. (Whether a particular radical survives secondary dissociation or not depends on how the total internal energy is partitioned between vibrational energy, which can be used to surmount the barrier, and rotational energy, which cannot.) Substitution of the central hydrogen with deuterium yields allyl radical fragments stable to dissociation at energies 2–3 kcal/mol greater than the nondeuterated allyl radical. This is somewhat surprising, as one would expect an increase in the allene+H product orbital angular momentum, $|\vec{L}|=\mu|\vec{v}_{rel}|b$, due to the increase in reduced mass, μ, leading to a reduction in the centrifugal barrier.

We attribute the increased stability in part to differing zero-point energies. Substitution of hydrogen with deuterium

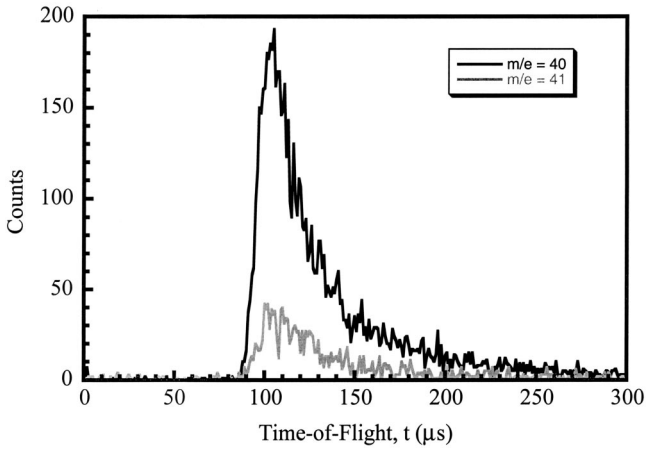

FIG. 9. A comparison of $m/e=40$ ($C_3H_4^+$, black line) corresponding to both direct [reaction (1)] and indirect [reaction (3)] allene formation and $m/e=41$ ($C_3H_3D^+$, gray line) corresponding to indirect propyne [reaction (2)] and allene [reaction (4)] time-of-flights from allyl-d_2 radical dissociation following photolysis of allyl-d_2 iodide at a source angle of 30° and a photoionization energy of 10.8 eV. Data were accumulated for 50 000 shots. As can be seen, $m/e=40$ allene formation dominates the $m/e=41$ allene/propyne contribution.

results in a lowering of the zero-point energy, which effectively leads to an increase in the barrier to allene+D formation over the barrier to allene+H formation of the nondeuterated radical. As described in the previous section, a comparison of allyl and allyl-d_2 radical zero-point energies predicts an increase of 1.5 kcal/mol in the barrier. However, the small magnitude of this increase in zero-point-corrected barrier height cannot alone account for the absence of expected centrifugal barrier lowering due to the increase of reduced mass experienced in these studies. Clearly, the zero-point isotope effect must work in combination with other factors.

Although reactions involving the loss of a deuterium atom rather than a hydrogen atom experience a decreased tunneling rate, it is an unlikely candidate to explain our observed increase in allyl-d_2 radical stability. First, it is doubtful that tunneling plays a major role in the dissociation reaction, as tunneling should decrease with decreasing energetic symmetry of the reaction. As the reaction of interest has a barrier[9] of 60 kcal/mol with a reverse barrier of 5.6 kcal/mol, tunneling is not expected to be of importance here. As our allyl radical signal begins to arrive at 48 μs (ion-flight-time corrected), all dissociative allyl radicals would have done so before detection, even those with lower tunneling rates. Thus, a decrease in reaction rate upon substitution of a D atom due to tunneling effects is most likely not responsible for the observed allyl radicals that are stable 48 μs after the primary dissociation.

A likely explanation for the improved stability of the allyl-d_2 radical lies in the lowered frequencies of the C–D bending modes. As the states with zero or one quanta in C–D bending of the allyl-d_2 radical lie lower in the potential well than the corresponding state of the nondeuterated radical, there should be a smaller range of impact parameters available to the relevant allyl-d_2 radicals with low excess vibrational energy and high rotational energies. This reduced range of impact parameters could then offset the gain in allene+H product angular momentum expected from the increase in reduced mass and ultimately increase the centrifugal barrier by the ~2 kcal/mol observed here.

A crude model was used to calculate the partitioning of rotational energy in the primary photolysis step. If the angular momentum of the parent allyl iodide molecule is taken to be negligible, then $\vec{L} \approx -\vec{J}$, where $\vec{L}$ is the orbital angular momentum from the nonzero impact parameter between the departing nascent allyl radical and iodine products and $\vec{J}$ is the angular momentum of allyl radical rotation. This approximation assumes an impulsive force along the C–I bond produces allyl radical rotation about an axis that intersects the C_3H_5 center-of-mass and is perpendicular to the plane formed by the C–I bond and a vector from the halogenated carbon to the C_3H_5 center-of-mass at the calculated[15] gauche equilibrium geometry of allyl iodide. The center-of-mass used for allyl radical rotation was taken as the center-of-mass of the C_3H_5 fragment frozen at its geometry in allyl iodide rather than the equilibrium geometry of the allyl radical. The most probable impact parameter predicted by this model of 1.12 Å (nondeuterated allyl iodide dissociation) and 1.13 Å (allyl-d_2 iodide dissociation) would result in 19 kcal/mol and 19.9 kcal/mol being partitioned to rotation for the nondeuterated allyl radical and allyl-d_2 radical, respectively, when 24 kcal/mol is partitioned to product translation. This slight increase in rotational energy of the allyl-d_2 radical would also contribute to the increased stability of the deuterated species.

The comparison of $m/e=40$ to $m/e=41$ spectra from the photodissociation of allyl-d_2 iodide gave a $m/e=40{:}41$ ratio of 4.5, and the photoionization cross section of allene[16] and propyne[17] are known to be similar at 10.8 eV. However, as shown in reactions (1)–(4), there is more than one possible way to obtain each mass, prohibiting a determination of the allene:propyne branching ratio. Allene detected at $m/e=40$ can be produced through two mechanisms: direct formation [reaction (1)] and the loss of deuterium following isomerization to the 2-propenyl radical [reaction (3)]. Allene and propyne can both be found at $m/e=41$, following the loss of one of two possible hydrogen atoms after isomerization to the 2-propenyl radical [reactions (2), (4), respectively]. There are therefore two possible ways to produce $m/e=40$ and four possible ways to make $m/e=41$. One must also consider isotope effects in the competition between reactions (3) and (4). There is a possible increase in the deuterium loss barrier [reaction (3)] due to zero-point effects, making quantitative analysis even more difficult.

One can also consider the effect of cyclization of the allyl radical, which has a barrier height of 52.7 kcal/mol.[5] The barrier for cyclopropyl radical→cyclopropene+H is 52.1 kcal/mol (81.7 kcal/mol above the allyl radical[5]). This is not energetically allowed for the $I(^2P_{1/2})$ formation channel, however, as E_{avl} is 83.6 kcal/mol. The E_{avl} for the $I(^2P_{3/2})$ formation channel products is 105.3 kcal/mol, leaving an internal energy range of $66.9 < E_{avl} < 105.3$ kcal/mol. If cyclopropene formation were considerable, one would need to truncate the $P(E_T)$ derived from the forward convolution fit to the $m/e=127$ spectrum to obtain a satisfactory fit to the $m/e=40$ data. As the $m/e=40$ momentum matches without any truncation of the $P(E_T)$ derived from the forward convolution fit to the $m/e=127$ spectrum taken with 200 eV electron-impact ionization[7] to accommodate those radicals with $E_{int} < 81.7$ kcal/mol, cyclopropene formation is ruled out.

Isotopic scrambling could be present if H atom migration in the cyclopropyl radical were favorable, as ring opening to form the allyl radical would now leave a H atom on the central carbon. This is doubtful, however, as the barrier to H atom migration lies up to 45.4 kcal/mol above the cyclopropyl radical (75 kcal/mol above the allyl radical[5]). Therefore, any cyclopropyl radicals formed should isomerize back to the allyl radical without isotopic scrambling and then dissociate, forming allene+D, allene-d_1+H or propyne-d_3 +H. Although it is not possible to determine an allene:propyne branching ratio, it is evident that allene formation is highly favored over propyne formation, in agreement with the previous PIE curve assessment.[7] The appearance of allene/propyne found at $m/e=41$ shows that some of the allyl radicals do isomerize to the 2-propenyl radical before dissociation. Although the results are not directly comparable to those of Deyerl *et al.*,[5] who used UV excitation of rota-

tionally cold allyl radicals, it is clear in these experiments that both the barrier to allyl radical dissociation and the barrier to isomerization are increased by centrifugal effects.

ACKNOWLEDGMENTS

This work was supported by the Division of Chemical Sciences, Office of Basic Energy Sciences, Office of Energy Research, U.S. Department of Energy, under Grant No. DE-FG02-92ER14305 (L.J.B.). The Chemical Dynamics Beamline is supported by the Director, Office of Science, Office of Basic Energy Sciences, Chemical Sciences Division of the U.S. Department of Energy under Contract No. DE-AC03-76SF00098. The ALS facility is supported by the Director, Office of Science, Office of Basic Energy Sciences, Materials Sciences Division of the U.S. Department of Energy, under the same contract. We would like to thank Professor G. Hillhouse for providing M.J.M. with hood space and to his graduate student, R. Waterman, for his assistance to M.J.M. in the allyl-d_2 iodide synthesis, and A. Unni for further assistance.

[1] H.-J. Deyerl, T. Gilbert, I. Fischer, and P. Chen, J. Chem. Phys. **107**, 3329 (1997).
[2] D. Stranges, M. Stemmler, X. Yang, J. D. Chesko, A. G. Suits, and Y. T. Lee, J. Chem. Phys. **109**, 5372 (1998).
[3] T. Schultz, J. S. Clarke, T. Gilbert, H.-J. Deyerl, and I. Fischer, Faraday Discuss. **115**, 17 (2000).
[4] J. Niedzielski, J. Gawlowski, and T. Gierczak, J. Photochem. **21**, 195 (1983).
[5] H.-J. Deyerl, I. Fischer, and P. Chen, J. Chem. Phys. **110**, 1450 (1999).
[6] I. Fischer and P. Chen, J. Phys. Chem. A **106**, 4291 (2002).
[7] D. E. Szpunar, M. L. Morton, L. J. Butler, and P. M. Regan, J. Phys. Chem. B **106**, 8086 (2002).
[8] J. A. Mueller, B. F. Parsons, L. J. Butler, F. Qi, O. Sorkhabi, and A. G. Suits, J. Chem. Phys. **114**, 4505 (2001).
[9] S. G. Davis, C. K. Law, and H. Wang, J. Phys. Chem. A **103**, 5889 (1999).
[10] *NIST Chemistry WebBook, NIST Standard Database Number 69*, National Institute of Standards and Technology, Gaithersburg, MD 20899, July 2001.
[11] X. Yang, J. Lin, Y. T. Lee, D. A. Blank, A. G. Suits, and A. M. Wodtke, Rev. Sci. Instrum. **68**, 3317 (1997).
[12] N. R. Daly, Rev. Sci. Instrum. **31**, 264 (1960).
[13] D. Peterka and M. Ahmed (private communication, 2002).
[14] D. W. Minsek and P. Chen, J. Phys. Chem. **97**, 13375 (1993).
[15] B. F. Parsons, D. E. Szpunar, and L. J. Butler, J. Phys. Chem. A **104**, 10669 (2000).
[16] D. M. P. Holland and D. A. Shaw, Chem. Phys. **243**, 333 (1999).
[17] J. C. Person and P. P. Nicole, J. Chem. Phys. **53**, 1767 (1970).